

## A 9 keV electron-impact liquid-gallium-jet x-ray source

M. Otendal,<sup>a)</sup> T. Tuohimaa, U. Vogt, and H. M. Hertz

*Biomedical and X-Ray Physics, Department of Applied Physics, Royal Institute of Technology/Albanova, SE-10691 Stockholm, Sweden*

(Received 20 August 2007; accepted 19 December 2007; published online 16 January 2008)

We demonstrate a high-brightness compact 9 keV electron-impact microfocus x-ray source based on a liquid-gallium-jet anode. A  $\sim 30$  W, 50 kV electron gun is focused onto the  $\sim 20$  m/s, 30  $\mu\text{m}$  diameter liquid-gallium-jet anode to produce an  $\sim 10$   $\mu\text{m}$  full width at half maximum x-ray spot. The peak spectral brightness is  $>2 \times 10^{10}$  photons/(s mm<sup>2</sup> mrad<sup>2</sup>  $\times$  0.1% BW). Calculation and experiments show potential for increasing this brightness by approximately three orders of magnitude, making the source suitable for laboratory-scale x-ray crystallography and hard x-ray microscopy. © 2008 American Institute of Physics. [DOI: 10.1063/1.2833838]

The high brightness of synchrotron sources has enabled a significant growth of crystallography and microscopy in the  $\sim 10$  keV range.<sup>1</sup> Laboratory systems for such studies commonly rely on 8 keV emission from copper rotating-anode x-ray sources. The image quality of the laboratory systems is limited by the low brightness of the compact x-ray source. In the present paper we describe a compact liquid-gallium-jet-anode electron-impact microfocus source with potential for three orders of magnitude higher brightness than present compact sources in this energy range.

In electron-impact sources a multi-keV electron beam strikes a solid metal anode to produce x-rays via bremsstrahlung and line emission. The x-ray brightness basically scales with the electron-beam power density on the anode. The major factor limiting the brightness is the thermal load capacity of the anode since  $\sim 99\%$  of the kinetic energy of the electron beam is converted into heat.<sup>2</sup> For microfocus x-ray tubes with circular foci (typically less than few tens of micrometers in diameter) the maximum  $e$ -beam power loading is in the range of 0.4–0.8 W per electron-beam diameter in micrometers [full width at half maximum (FWHM) of Gaussian beam].<sup>3</sup> This corresponds to an  $e$ -beam power density at the anode of approximately 25–50 kW/mm<sup>2</sup> for a 10  $\mu\text{m}$  source. For comparison, larger-spot systems based on modern rotating anodes are limited to 10–20 kW/mm<sup>2</sup> for short exposures while large-spot stationary anodes usually operate at 1 kW/mm<sup>2</sup>. These numbers are not likely to increase significantly.<sup>4</sup> Angled viewing of a line focus can increase the apparent, but not the actual, power density for large-spot geometries.

Here we demonstrate a 9 keV compact microfocus source which shows promise for three orders of magnitude higher brightness than present compact sources by operating at very high  $e$ -beam power density. This source is based on a liquid-gallium-jet anode and the spectrum is dominated by gallium line emission at 9.3 keV. The high  $e$ -beam power density capacity of this anode type is, in short, due to the different thermal properties of liquid-gallium versus solid-metal anodes and the possibility of a much higher anode

speed with a liquid-jet anode. In addition and in contrast to existing techniques, the gallium-jet anode is completely regenerative and is therefore not as sensitive to anode damage as solid anodes. Electron-impact sources based on liquid-jet anodes have previously been demonstrated for 25 keV line emission using solder<sup>5,6</sup> and tin.<sup>7</sup> The high spatial coherence of this source allowed short-exposure-time x-ray phase imaging.<sup>8</sup> Gallium jets have been used as targets for femto-second laser plasma 9 keV emission, although with much lower average brightness.<sup>9</sup>

Figure 1 shows the experimental arrangement. It consists of a gallium-filled stainless-steel pressure tank, which is placed inside an IR-radiation oven used to raise the temperature to  $\sim 50$  °C. This is well above the melting point of gallium (29.8 °C). The pressure tank is placed in a vacuum chamber, which is typically pumped down to a  $\sim 10^{-4}$  mbar during the experiments. By applying up to 200 bars of nitrogen backing pressure, the molten gallium is ejected as a liquid jet into the vacuum chamber through a tapered glass nozzle with a 30  $\mu\text{m}$  orifice. The electron-beam system can be operated at acceleration voltages up to 50 kV and is based on a 50  $\mu\text{m}$  diameter flat single-crystal LaB<sub>6</sub> cathode with a capacity of delivering up to  $\sim 2$  mA of current. Using a magnetic lens the electrons are focused onto the gallium jet, generating an x-ray spot with a FWHM down to 10  $\mu\text{m}$ . At right angles to both the  $e$ -beam and the metal jet there is an x-ray detector with a CdZnTe diode used for quantitative spectral characterization of the source. For measurements of the source size, the diode is exchanged for a  $36 \times 24$  mm<sup>2</sup> x-ray charge coupled device (CCD) detector ( $4008 \times 2672$ ,  $9 \times 9$   $\mu\text{m}^2$  pixels) which images a 20  $\mu\text{m}$  thick sharp gold edge. By deconvolution of the edge image the edge-spread function of the source may be determined and used for calculation of the FWHM of the x-ray spot.

The quantitative x-ray spectral brightness of the source is determined by combining the CdZnTe-diode spectral measurements with the source-size measurements. Figure 2 shows the calibrated x-ray spectrum generated when a 34 W (50 kV, 0.68 mA) electron-beam interacts with a 30  $\mu\text{m}$  diameter,  $\sim 20$  m/s gallium jet. In this experiment the FWHM diameter of the approximately Gaussian x-ray spot was determined to  $\sim 15$   $\mu\text{m}$ . The corresponding quantitative spec-

<sup>a)</sup>Electronic mail: mikael.otendal@biox.kth.se.

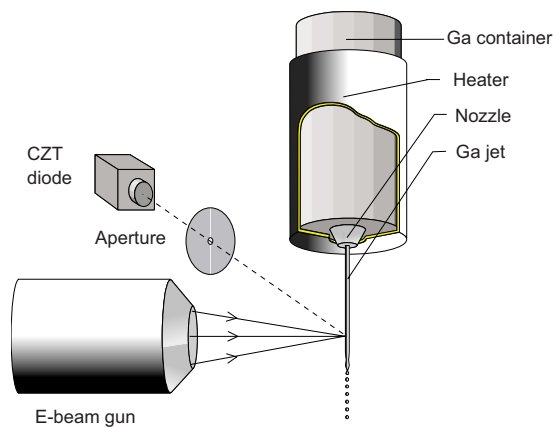


FIG. 1. (Color online) The experimental arrangement for the liquid-gallium-jet anode x-ray source.

tral brightness was determined with the CdZnTe diode for the bremsstrahlung and the Ga  $K\alpha$  peak in Fig. 2 is  $3 \times 10^6$  and  $1.4 \times 10^8$  photons/(s mm<sup>2</sup> mrad<sup>2</sup>  $\times$  0.1% BW), respectively. Given the  $\sim 600$  eV spectral bandwidth of the diode the  $K\alpha$  line brightness is  $9 \times 10^9$  photons/(s mm<sup>2</sup> mrad<sup>2</sup>). Due to the natural line width of  $\sim 2.6$  eV of the doublet Ga  $K\alpha$  line<sup>10</sup> the peak spectral brightness is  $2.2 \times 10^{10}$  photons/(s mm<sup>2</sup> mrad<sup>2</sup>  $\times$  0.1% BW) (2:1 ratio between  $K\alpha_1$  and  $K\alpha_2$ ). A quasimonochromatic 9.3 keV source is obtained by inserting, e.g., a 10  $\mu$ m thick Zn filter, which attenuates the main  $K\alpha$  line by 25% and the weaker  $K\beta$  by line 80%.

The highest x-ray brightness, expressed in  $e$ -beam power per x-ray spot size, recorded in the present experiments was  $\sim 170$  kW/mm<sup>2</sup> (27 W  $e$ -beam power and 10  $\mu$ m FWHM x-ray spot). Since the  $e$ -beam spot is smaller than the x-ray spot due to, e.g., electron scattering in the anode, we can estimate the  $e$ -beam power loading to be  $\geq 3$  W/ $\mu$ m. This number is four to eight times higher than those for solid-anode microfocus sources, see above. Thus, the performance of our proof-of-principle arrangement is already significantly better than those for presently commercially available

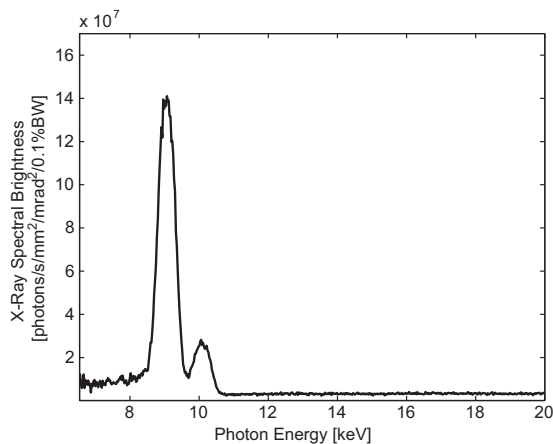


FIG. 2. Calibrated x-ray spectrum from the liquid-gallium-jet anode. The raw spectrum has been compensated for absorption in the air and the beryllium window along with corrections regarding the spot size, exposure time, photon energies, and detector efficiency. The two peaks are the  $K\alpha$  and the  $K\beta$  lines at 9.3 and 10.3 keV, respectively.

sources. All data in the experiments were obtained with moderate heating of the jet (see below) resulting in negligible debris emission. In the next two paragraphs we show that the source can be operated at approximately 100 times higher power density by increasing the speed and the heating of the jet, thereby reaching the cathode- and lens-limited  $e$ -beam power density of a few tens of MW/mm<sup>2</sup> for focused electron-optical systems in the 10–1000 W range.<sup>11,12</sup>

Increasing the speed of the jet allows a correspondingly higher power density on the jet without an increase in temperature of the x-ray spot. This requires a stable high-speed gallium jet. In short, the stability of liquid jets can be characterized by the following four fluid mechanical parameters:<sup>13,14</sup> the Reynolds number ( $Re = \rho v d / \mu$ ), the Ohnesorge number ( $Z = \mu / \sqrt{\rho \sigma d}$ ), the atmospheric Weber number ( $We_A = \rho_A v^2 d / \sigma$ ), and the Mach number ( $Ma = v / c$ ), where  $\rho$ ,  $\mu$ , and  $\sigma$  are the density, viscosity and the surface tension of the jet liquid, respectively,  $d$  is the jet diameter,  $v$  is the speed of the jet,  $c$  is the speed of sound in the jet liquid, and  $\rho_A$  is the density of the surrounding atmosphere. It has previously been shown that it is possible to operate a stable and well collimated water jet in vacuum with the following parameters:  $Re = 5.6 \times 10^4$ ,  $Z = 4.7 \times 10^{-3}$ ,  $We_A \sim 4.6$ , and  $Ma = 0.08$  at a vacuum pressure of 50 mbars ( $\rho_A \sim 6 \times 10^{-2}$  kg/m<sup>3</sup>).<sup>15</sup> According to the theory of dynamical similarity<sup>16</sup> any jet that matches these numbers will behave in a similar manner. Assuming a gallium jet in a  $10^{-4}$  mbar vacuum environment with the following parameters  $v = 520$  m/s,  $d = 30$   $\mu$ m,  $T = 75$   $^\circ$ C,  $\rho = 6.1 \times 10^3$  kg/m<sup>3</sup>,  $\sigma = 0.71$  N/m,  $\mu = 1.7 \times 10^{-3}$  N s/m<sup>2</sup>, and  $c = 2740$  m/s, this will result in  $Re = 5.6 \times 10^3$ ,  $Z = 4.7 \times 10^{-3}$ ,  $We_A \sim 10^{-6}$ , and  $Ma = 0.19$ . The slight difference between the  $Ma$  for the water and gallium jets can be disregarded, since for values of  $Ma < 0.3$  the fluid is considered to be in an uncompressed state.<sup>14</sup> Furthermore, for  $We_A < 5.3$  it has been proven that the ambient atmosphere does not influence the breakup or the stability of a liquid jet.<sup>17</sup> Thus, it should be possible to generate a gallium jet at more than 20 times higher speed than the jet used in this paper. Such a fast jet would operate at the same spot temperature as in the present experiments at 20 times increased power density.

The thermal properties of the gallium jet allow a further increase in power density. Assuming that the full jet is uniformly heated by the electron beam the temperature increase  $\Delta T$ , can be estimated using the following formula:

$$\Delta T = \frac{4P_{\text{abs}}}{\pi d^2 v \rho c_p}, \quad (1)$$

where  $P_{\text{abs}}$  is the absorbed electron-beam power in the jet and  $c_p$  is the specific heat capacity of the jet liquid. Since about a third of the electrons are backscattered as it strikes the jet surface not all of the electron-beam power contributes to increasing the jet temperature. A Monte Carlo simulation<sup>18</sup> shows that about 80% of the  $e$ -beam power heats the jet, which results in a jet temperature of  $\sim 700$   $^\circ$ C when applying the simplified model of Eq. (1) on the 27 W/10  $\mu$ m configuration mentioned above. However, given the limited electron penetration depth (4–5  $\mu$ m) (Ref. 18) the local focus-spot temperature may be higher. To simulate the temperature of the gallium jet using this more realistic  $e$ -beam power distribution a finite element calculation was made.

This resulted in a peak temperature on the jet surface of approximately 800 °C, which is close to the boiling point of gallium given the  $\sim 10^{-4}$  mbar vacuum pressure. This surprisingly small increase of surface temperature is due to the fact that the electron-beam energy deposition peak is located a few microns below the jet surface. The simulation also showed significant heat dissipation in the jet after the interaction with the  $e$ -beam. The combination of these features suggests that there should be a negligible amount of debris emission from the jet, which is also in good agreement with the experimental observations.

Finally, we note that the increase in apparent electron power density due to angled viewing of a line focus (used in solid-anode x-ray tubes) can be applied to the liquid-gallium-jet anode as well. In the present experiments, the approximately Gaussian  $e$ -beam spot interacts with a cylinder-shaped jet. The observed x-ray spot is elliptical with FWHM values of  $10 \times 8 \mu\text{m}^2$ , i.e., a gain in effective power density of only a factor of 1.25. This should be compared to solid-anode tubes that use a line-shaped focus and a takeoff angle of  $6^\circ$ – $12^\circ$ , which yields an effective source area decrease by a factor of 5–10. However, by having a flat or large-diameter gallium jet (in comparison with the FWHM of the  $e$ -beam spot) a similar improvement in the effective power density may be achieved for gallium-jet-anode sources as for the solid-anode tubes.

With the scaling discussed above (increased jet speed,  $\sim 20\times$ ; complete vaporization of jet,  $\sim 10\times$ ; better utilization the line-focus principle, 5– $10\times$ ) the peak spectral brightness at the 9.3 keV  $K\alpha$  line would be on the order of  $10^{13}$  photons/(s mm<sup>2</sup> mrad<sup>2</sup>  $\times$  0.1% BW), only one to two orders of magnitude lower than that of present bending-magnet synchrotron sources. This makes the liquid-gallium-jet source a suitable candidate for laboratory-scale x-ray crystallography and hard x-ray microscopy. Low- and medium-resolution crystallography is presently done with compact sources<sup>19</sup> while applications requiring high-resolution, high signal-to-noise, and/or small sample volumes must be performed at high-brightness synchrotron facilities.<sup>1</sup> Here the brightness of the liquid-gallium-jet source may enable several of the high-end applications to be performed locally. Interestingly, the increased need for automatization, throughput, and rapid in-house screening in protein crystallography has recently motivated the development of an in-house “compact” synchrotron light source, which, in combination with new miniaturized sample preparation methods, shows promise for a streamlined gene-to-structure pathway.<sup>20</sup> Naturally, the liquid-gallium-jet source would also improve exposure times in present laboratory crystallography systems based on rotating anodes.<sup>19</sup> Along

the same line of arguments, the source may make hard x-ray microscopy presently performed at synchrotron radiation facilities feasible in the small-scale laboratory and reduce exposure times of present rotating-anode-based compact x-ray microscopy systems.<sup>21</sup>

In summary, we have operated a compact electron-impact liquid-gallium-jet anode hard-x-ray source at an electron-beam power loading close to an order of magnitude higher than what is available today. The source has potential to increase the x-ray brightness three orders of magnitude compared to present compact sources, thereby significantly reducing the gap to bending-magnet synchrotron sources and making it suitable for in-house x-ray crystallography and microscopy.

This work has been supported by the Swedish Agency for Innovation Systems, the Swedish Foundation for Strategic Research, and the Swedish Science Research Council.

<sup>1</sup> See, e.g., J. Als-Nielsen and D. McMarrow, *Elements of Modern X-Ray Physics* (Wiley, New York, 2004); www.esrf.fr

<sup>2</sup> E. Krestel, *Imaging Systems for Medical Diagnostics* (Siemens, Berlin, 1990).

<sup>3</sup> D. E. Grider, A. Wright, and P. K. Ausburn, *J. Phys. D* **19**, 2281 (1986).

<sup>4</sup> E. Ammann and W. Kutschera, *Br. J. Radiol.* **70**, S1 (1997).

<sup>5</sup> O. Hemberg, M. Otendal, and H. M. Hertz, *Appl. Phys. Lett.* **83**, 1483 (2003).

<sup>6</sup> O. Hemberg, M. Otendal, and H. M. Hertz, *Opt. Eng.* (Bellingham) **43**, 1682 (2004).

<sup>7</sup> M. Otendal, T. Tuohimaa, O. Hemberg, and H. M. Hertz, *Proc. SPIE* **5537**, 57 (2004).

<sup>8</sup> T. Tuohimaa, M. Otendal, and H. M. Hertz, *Appl. Phys. Lett.* **91**, 074104 (2007).

<sup>9</sup> G. Korn, A. Toss, H. Stiel, U. Vogt, M. Richardsson, and T. Elsaesser, *Opt. Lett.* **27**, 866 (2002).

<sup>10</sup> M. O. Krause and J. H. Oliver, *J. Phys. Chem. Ref. Data* **8**, 329 (1979).

<sup>11</sup> T. Tuohimaa, M. Otendal, and H. M. Hertz, *Proc. SPIE* **5918**, 225 (2005).

<sup>12</sup> M. Otendal, T. Tuohimaa, and H. M. Hertz, *J. Appl. Phys.* **101**, 026102 (2007).

<sup>13</sup> S. P. Lin and R. D. Reitz, *Annu. Rev. Fluid Mech.* **30**, 85 (1998).

<sup>14</sup> R. D. Blevins, *Applied Fluid Dynamics Handbook* (Krieger, Malabar, FL, 1992), pp. 10–12.

<sup>15</sup> M. Otendal, O. Hemberg, T. T. Tuohimaa, and H. M. Hertz, *Exp. Fluids* **39**, 799 (2005).

<sup>16</sup> J. F. Douglas, J. M. Gasiorek, and J. A. Swaffield, *Fluid Mechanics*, 3rd ed. (Longman Scientific & Technical, Singapore, 1995), pp. 262–267.

<sup>17</sup> R. W. Fenn III and S. Middleman, *AIChE J.* **15**, 379 (1969).

<sup>18</sup> A. Couture and D. Drouin, *Casino*, www.gel.usherbrooke.ca/casino/ (2002).

<sup>19</sup> M. Gubarev, E. Ciszak, I. Ponomarev, W. Gibson, and M. Joy, *J. Appl. Crystallogr.* **33**, 882 (2000).

<sup>20</sup> M. K. Yadav, C. J. Gerds, R. Sanishvili, W. W. Smith, L. S. Roach, R. F. Ismagilov, P. Kuhn, and R. C. Stevens, *J. Appl. Crystallogr.* **38**, 900 (2005); http://www.atcg3d.org/technologies.htm

<sup>21</sup> See, e.g., www.esrf.fr and www.xradia.com